

# MgO/GaSe<sub>0.5</sub>S<sub>0.5</sub> Heterojunction as Photodiodes and Microwave Resonators

Atef F. Qasrawi, Hazem K. Khanfar, *Member, IEEE*, and N. M. Gasanly

**Abstract**—In this paper, a multifunctional operating optoelectronic device that suits visible light (VLC) and microwave communication systems is designed and characterized. The device which is composed of p-type MgO and n-type GaSe<sub>0.5</sub>S<sub>0.5</sub> heterojunction is characterized by means of optical absorbance in the incident light energy ( $E$ ) region of 3.5–1.1 eV, dark and illuminated current ( $I$ )–voltage ( $V$ ) characteristics, and impedance spectra in the frequency range of 1M–1.8 GHz. Four types of lasers which generate light of wavelengths 406, 632, 850, and 1550 nm are used to excite the active region of the device. The device was also illuminated by non-monochromatic light. The incident light power was varied in the range of 1.12–10.17  $\mu$ W. It was observed that the heterojunction exhibits an optical energy bandgap ( $E_g$ ) of 1.85 eV. For laser excitation with  $E > E_g$ , the photosensitivity ( $S$ ) exceeds 67 while it is less than unity for excitations with  $E < E_g$ . These behaviors are assigned to the intrinsic and extrinsic nature of absorption, respectively. In addition,  $S$  increases as a result of energy barrier height lowering with increasing light power. On the other hand, when the device was excited with ac signal, the capacitance and impedance of the device displayed a resonance–antiresonance property associated with negative differential resistance and very high signal quality factor ( $10^3$ ) above 1.37 GHz. The bandwidth of the two resonance–antiresonance peaks is 319 and 12.6 MHz at 1.475 and 1.649 GHz, respectively. These results are attractive for using the heterojunction in VLC and microwave communication technologies.

**Index Terms**—Optical materials, heterojunction, impedance spectroscopy, microwave.

## I. INTRODUCTION

RECENT developments in the sector of visible light communication technology (VLC) appear to be promising as significant records on optical data transfer are achieved. A 550 Mbit/s real-time VLC system based on nonreturn-to-zero on-off keying (NZR-OOK) modulation of a white light (LED) is reported [1]. The system which gets use from

Manuscript received September 2, 2015; accepted September 15, 2015. Date of publication October 2, 2015; date of current version January 12, 2016. This work was supported by the Ministry of Higher Education within the State of Palestine through the Project entitled Design and Characterization of MgO/GaSe<sub>0.5</sub>S<sub>0.5</sub> Multifunctional Resonant Microwave Optoelectronic Sensors under Grant 2/1/2013. The associate editor coordinating the review of this paper and approving it for publication was Prof. M. N. Abedin.

A. F. Qasrawi is with the Department of Physics, Arab American University–Jenin, Jenin 240, Palestine, and also with the Group of Physics, Faculty of Engineering, Atilim University, Ankara 06836, Turkey (e-mail: atef.qasrawi@atilim.edu.tr).

H. K. Khanfar is with the Department of Telecommunication Engineering, Arab American University–Jenin, Jenin 240, Palestine (e-mail: hazem.khanfar@aaup.edu).

N. M. Gasanly is with the Department of Physics, Middle East Technical University, Ankara 06800, Turkey (e-mail: nizami@metu.edu.tr).

Digital Object Identifier 10.1109/JSEN.2015.2486000

n-p-n transistors exhibit a 3-dB bandwidth of VLC link that covers a frequency domain from 3 to 233 MHz with the help of a blue-filter. Such types of systems are improved to reach a 614 Mbit/s by using the duobinary technique visible LED through post-equalizing circuits with simple RC networks [2]. The VLC signal receivers are made of various types of optoelectronic devices. Examples of these devices include organic bulk heterojunction photodetector which is made of poly(3-hexylthiophene) (P3HT) and phenyl C61-butyric acid methyl ester (PCBM) as the active layer. This system displayed a responsivity of 0.18 A/W and a modulation response of 790 kHz at  $-6$  V [3]. Another p-n heterojunction made of rutile TiO<sub>2</sub> nanorod arrays on p-Si (111) is reported to display a 106 mA/W as exposed to 395 nm light pulses [4].

One of the promising materials that are used in visible light photo-detecting is the GaSe<sub>1-x</sub>S<sub>x</sub> thin crystals and the MgO in thin film form [5]–[8]. The Ni/MgO/Au photovoltaic devices displayed a photovoltaic effect presented by an open circuit voltage of 0.12–0.47 V, short circuit current density of 3.9–10.5  $\mu$ A/cm<sup>2</sup>, quantum efficiency of 0.662–0.052, and responsivity of 0.179–0.024 A/W under photoexcitation optical power of 2.2–28.2  $\mu$ W [5]. On the other hand, the design of the back-to-back C/GaSe<sub>0.5</sub>S<sub>0.5</sub>/C Schottky device is reported to reduce the dark current of the normal Ag/GaSe<sub>0.5</sub>S<sub>0.5</sub>/C Schottky diode by 13 times and increased the photosensitivity from 3.8 to  $2.1 \times 10^3$  [6]. Alternatively, when a p-n heterojunction is made of MgO/Ga<sub>4</sub>Se<sub>3</sub>S and subjected to a 632.5 nm laser radiation of 3.0 mW, the heterojunction responsivity reached a value of 80 [7]. In a double heterojunction design made of mixed-phase of MgZnO/i-MgO/p-Si the distinct dominant responses at solar blind (250 nm) and visible blind (around 330 nm) UV regions under different reverse biases are detected [8]. The Ni/MgO/Au, the C/GaSe<sub>0.5</sub>S<sub>0.5</sub>/C, and the MgO/Ga<sub>4</sub>Se<sub>3</sub>S [5]–[7] structures are also reported to exhibit good characteristics that nominate it as microwave resonators which can be used in microwave communication technology. For this reason, here in this work, we aim to discuss the design of the Ag/MgO/GaSe<sub>0.5</sub>S<sub>0.5</sub> (Ag, C) hybrid device that can handle the visible light communication duty through photodetecting and the ac signal amplification/absorption at microwave frequencies.

In our previous work [9] we have discussed the physical variations associated with the design of the MgO/GaSe<sub>0.5</sub>S<sub>0.5</sub> interface. Particularly, the effects of the MgO interfacing on the crystal structure, on the crystal's optical reflectivity, absorbability, valence band splitting and dielectric property are explored. In addition, a specific application guidance presented

by the current-voltage characteristics in the dark and under laser light excitation of 406 nm is discussed. It was observed for pure sodium silicate and for a 67% content of MgO solved in sodium silicate binder (33%), the heterojunction exhibits a valence band shift of 0.40 and 0.70 eV, respectively. While the angle-dependent reflectance measurements on the crystal displayed a Brewster condition at 70°, the MgO/GaSe<sub>0.5</sub>S<sub>0.5</sub> heterojunction exhibited no Brewster condition when irradiated from the MgO side. On the other hand, the  $I - V$  characteristics of the device show current amplification of 24 times when irradiated with 5 mW power laser light. Following up with these results, here in this work, we study the effects of the intrinsic nature of absorption under laser excitation of 850 and 1550 nm as well as the extrinsic nature of absorption under laser excitation of 406 and 632 nm of on the photosensitivity of the device. In addition, the laser light intensity effects on the device's barrier height is reported. Moreover, the impedance spectra in the frequency range of 1.0 M-1.80 GHz which nominates the MgO/GaSe<sub>0.5</sub>S<sub>0.5</sub> heterojunction as microwave resonator is reported and analyzed.

## II. EXPERIMENTAL DETAILS

The n-type GaSe<sub>0.5</sub>S<sub>0.5</sub> crystals which were obtained by the Bridgman method from the stoichiometric melt of the starting materials were used as a substrate for the p-type MgO layer. The Bridgman method is employed as it guarantees the highly preferred orientation of the crystal and to reduce the defects associated with atomic migrations during the crystal growth. For optical measurements, the cleaved crystal and MgO layers were restricted to be of  $\sim d = 1.0$  and  $13.6 \mu\text{m}$  thick, respectively. The MgO paste, which was prepared by solving the MgO nano-powders (Alfa Aesar 99.99%) in a silicate binder (SiO<sub>2</sub>: Na<sub>2</sub>O<sub>2</sub>:CO<sub>3</sub>) was painted carefully on the surface of the crystals. For electrical measurements, the crystal and MgO layer's thickness was 0.27 and 0.40 mm, respectively. The separation between the MgO and carbon contact line was 1.24 mm. The total device area was  $\sim 6.1 \times 10^{-3} \text{cm}^2$ . The current-voltage characteristics were recorded using Keithley 230 voltage source and Keithley 6485 picoammeter. The light excitation was carried out using Thorlabs MCLS1 4-channel fiber-coupled laser source that can generate light at wavelengths of 406, 850 and 1550 nm. The He-Ne laser was also used to generate light of 632.5 nm. The impedance spectroscopy was recorded using Agilent 4291B 1.0 M-1.8 GHz impedance analyzer. The connections to the fixtures (the 16193A small side electrode, 16453A dielectric material test fixture, and Hp16192 A/70 side electrode test fixture) were made by AP-7 connector attached to the analyzer. The optical absorbance was recorded using thermo-scientific UV-VIS Evolution 300 spectrophotometer.

## III. RESULTS AND DISCUSSION

The geometrical design of the MgO/GaSe<sub>0.5</sub>S<sub>0.5</sub> optoelectronic device is shown in the inset of Fig. 1 (a). It is built so that it allows ac signal propagating between the two Ag contacts and the dc signal between the top Ag contact above the MgO layer and the carbon contact above the GaSe<sub>0.5</sub>S<sub>0.5</sub> crystal layer. The latter is designed so that it allows maximum

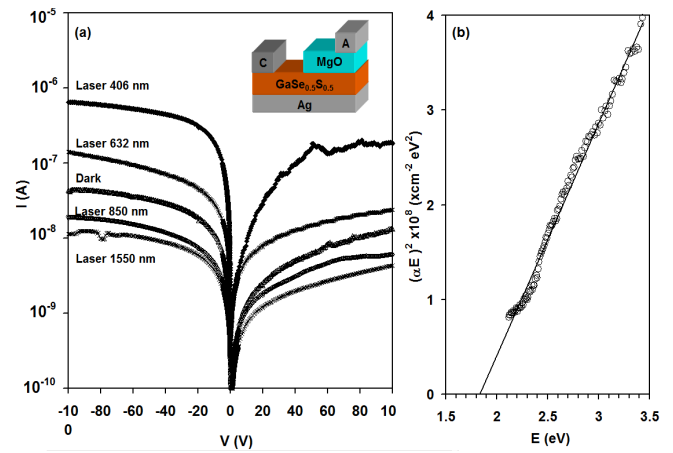


Fig. 1. (a) The current-voltage characteristics for the Ag/MgO/GaSe<sub>0.5</sub>S<sub>0.5</sub>/C device in the dark and under laser excitations. (b) The  $(\alpha E)^2 - E$  variations for the heterojunction. The geometrical design is shown in the inset of (a).

active region for light absorption. The resulting dark and laser illuminated current ( $I$ )-voltage ( $V$ ) characteristics are shown in Fig. 1 (a). The dark  $I - V$  characteristic is observed to exhibit larger reverse current than that of the forward one. The forward current is supplied from the carbon side which exhibits Schottky type of contact with the GaSe<sub>0.5</sub>S<sub>0.5</sub> crystal's surface [6], [10]. The barrier heights ( $\phi_b$ ), which are obtained from the data presented in Fig. 1(a), using the previously described method [10], is found to be 0.75 and 0.74 eV, for forward and reverse biased currents, respectively. The  $\sim 0.75$  eV barrier height value is higher than that we have previously determined as 0.65 eV for the Ag/GaSe<sub>0.5</sub>S<sub>0.5</sub>/C structure [10] and less than 0.84 eV which was reported for the back-to-back C/GaSe<sub>0.5</sub>S<sub>0.5</sub>/C Schottky device [6]. These slight attenuations could be probably assigned to the effect of the p-type charge carriers which recombine with some electrons when the p-type MgO layer is painted on the surface of the n-type crystal [14]. In accordance to the p-n junction interfacing theory which is described in [14], at the instant of pn interfacing, the holes which are at higher concentration in the p-region, flow to the n-region and the electrons in the n-region flow to the p-region causing the recombination process. The migrated holes and electrons leave behind uncompensated negatively and positively charged acceptor and donor ions, respectively. Some of which are left uncompensated as electrons diffuse from the n-side to the p-side. Thus, a double layer of charge is created near the junction having negative space charge on the p-side and positive space charge on the n-side and, as a result a built in field presents a barrier to the motion of majority carriers but aids the flow of minority carriers. The height of this barrier is controlled by the amount of uncompensated charges.

Fig. 1 (a) also displays the laser light excitation effects on the  $I - V$  characteristics of the device. The largest response of light appears for laser beam of 406 nm wavelength (3.06 eV); the light to the current ratio ( $S = I_{light}/I_{dark}$ ) is 15.4 at a biasing voltage of  $-5.0$  V. When the devices are irradiated with 632 nm (1.97 eV) He-Ne laser, the photosensitivity ( $S$ ) value lowers to 2.64. On the other hand, when the device was

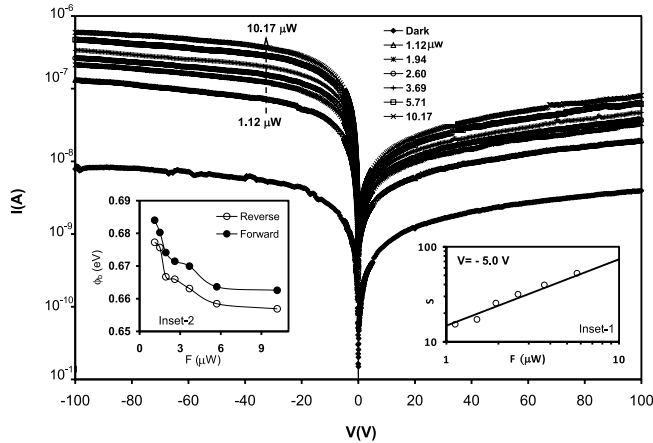


Fig. 2. The current-voltage characteristics of the heterojunction under the excitation power of non-monochromatic light. Inset-1 and inset-2 show the barrier height and the photosensitivity of the device as a function of excitation power, respectively.

excited with 850 nm (1.46 eV) and 1550 nm (0.80 eV) laser light, the photosensitivity values are less than unity indicating that the current decreased under illumination opposite to the 406 and 632 nm laser excitations. Such behavior of the device can be explained by means of extrinsic/intrinsic absorption phenomena which were described through the photo-excitation analysis of this work. The extrinsic absorption is caused by the impurities that are present in the materials [11]. Although the binder content is low compared to MgO in the films, the compositors of the binder which are C, Na and Si atoms play the role of impurities in the device. During the extrinsic absorption process, the electrons are transmitted from one energy level of these elements to another, causing a reduction in the total dark current, when excited with 850 and 1550 nm laser light, as a result of the electrons not being able to reach the conduction band directly; thus the photosensitivity of the device decreases. On the other hand, the absorption spectra which were recorded for a 13.6  $\mu\text{m}$  thick MgO/GaSe<sub>0.5</sub>S<sub>0.5</sub> bilayer and presented in Fig. 1 (b) revealed the direct energy band gap  $E_g = 1.85$  eV in accordance with the  $(\alpha E)^2 - E$  variation. This value represents a critical point of absorption evaluation. Namely, when laser light of energies greater than  $E_g$  is used to excite the device, the illuminated current is higher than the dark and the  $S$  values are larger than unity. Such behavior is clearly due to the intrinsic nature of absorption in which the electrons gain the sufficient energy to reach the conduction band and recombine directly with holes. For laser lights of energies less than  $E_g$  like the 850 and 1550 nm, the incident photon energy is not sufficient to allow the electrons reaching the conduction band and thus the extrinsic absorption dominates [11].

Fig. 2 represents the current-voltage characteristics of the device after being irradiated with the light of the wide band spectrum (tungsten lamp: maximum peak of the spectrum is  $\sim 2.14$  eV). The intensity of light is altered in the light power range of 1.12-10.17  $\mu\text{W}$ . As the figure displays, an excellent response to light is observed. The  $I - V$  characteristics of the Ag/MgO/GaSe<sub>0.5</sub>S<sub>0.5</sub>/C device shifts up indicating the generation of more electrons as the light intensity is increased.

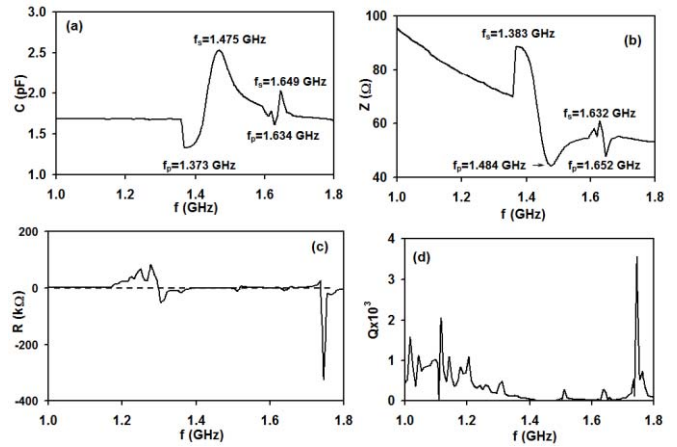


Fig. 3. (a) The capacitance, (b) the impedance, (c) the resistance and (d) the quality factor spectra for the device in the frequency range of 1.0-1.8 GHz.

The photosensitivity of light which was calculated for a biasing voltage of  $-5.0$  V is displayed in inset 1 of Fig. 2. As the inset shows,  $S$  increases with increasing illumination intensity ( $F$ ). The  $S - F$  variation can be presented by the power law,  $S = 14.8F^{0.7}$ . This relation is promising as it indicated that the more incident photons, the more generated photocurrent and the more sensitive the device. In order to understand the reasons that lay beyond the enhancement in the photosensitivity with increasing illumination power, the barrier height of the Ag/MgO/GaSe<sub>0.5</sub>S<sub>0.5</sub>/C device during the forward and reverse biasing conditions is calculated and plotted as a function of illumination power. The plots which are presented in inset-2 of Fig. 2, display a sharp decrease in the energy barrier height of the device with increasing light power. The same trend of behavior appears under both forward and reverse biasing conditions. Particularly, at reverse biased the barrier height decreases from 0.74 eV in the dark to 0.68 eV and reaches 0.66 eV when the light power is increased from 1.12 to 10.17  $\mu\text{W}$ , respectively. The decrease in the barrier height is ascribed to the increased density of electrons and holes that are associated with the increase in the photoexcitation power [12], [13]. The generated electrons and holes accumulate on the sides of the depletion region layer, causing some more electron-hole recombination that result in narrowing and lowering of the barrier. In addition, the nonlinear  $S - F$  variations indicate that the photo conduction is also affected by exponential trap distributions. The trap states that behave as sensitizing/recombination centers under photoexcitation lower the barrier height and result in larger photocurrent when the density of recombination and sensitizing centers is much larger than the density of free carriers available for conduction [15]. The optical pumping of these centers releases more carriers that support the conduction.

Fig. 3 (a)-(d) illustrates the results of the ac signal analyses for the Ag/MgO/GaSe<sub>0.5</sub>S<sub>0.5</sub>/Ag device being recorded at zero bias voltage in the frequency range of 1.0-1.8 GHz. As it is easily readable from Fig. 3 (a), the capacitance ( $C$ ) of the device is relatively low and oscillates in the range of 1.32-2.54 pF. The capacitance spectrum displays a resonance (series)-antiresonance (parallel) behavior at

two positions. While the parallel frequency ( $f_p$ ) appears at 1.373 and at 1.634 GHz, the series resonance ( $f_s$ ) appear at 1.475 and 1.649 GHz. The same behavior is also detectable from the magnitudes of the capacitive reactance ( $|X_c|$ ), resistance and the impedance ( $|Z|$ ) spectrum, which is presented in Fig. 3 (b). The  $f_p$  and  $f_s$  values are shifted from those observed for the  $C - f$  spectra due to the inverse relation between the capacitance and capacitive reactance. Since the values of  $X_c$  are much larger than those of  $R$ . The impedance is mainly governed by the capacitive part. This behavior is easily observed in Fig. 3(b). The respective inductive region presented by the frequency difference  $\Delta f = |f_s - f_p|$ , is 102 and 15 MHz for the first and second resonance-antiresonance positions, respectively. In addition, Fig. 3 (c) displays the resistive part of the impedance spectrum. The resistance exhibits negative values in the regions of 1.301-1.522 GHz and 1.623-1.653 GHz. The negative resistance happens due to the charge transfer between the material which has high charge carriers and the one which has low concentration. This may have occurred during the charge transfer between the Ag metal and the MgO layer ( $p = 10^{16} \text{ cm}^{-3}$  [7]) or the metal and the GaSe<sub>0.5</sub>S<sub>0.5</sub> layer ( $n = 10^{12} \text{ cm}^{-3}$  [6]) and during transfer between the p-n layers. In this process filled conduction band states overlap in energy with empty valence band states, permitting tunneling and leading to negative differential resistance [16].

On the other hand, the quality factor ( $|Q|$ ) of the signal is displayed in Fig. 3 (d). As seen from this figure, the quality factor exhibits values that could reach  $3.56 \times 10^3$  at 1.746 GHz. The series resonance peak bandwidth ( $f_s/Q$ ) is 319 and 12.6 MHz for  $f_s$  values of 1.475 and 1.649 GHz, respectively.

The resonance-antiresonance behavior of the Ag/MgO/GaSe<sub>0.5</sub>S<sub>0.5</sub>/Ag device can be explained by the four parameter crystal model [17] which assumes that the device is composed to two parallel arms. Namely, the static arm which consists of a single capacitance  $C_0$  (shunt capacitance) and the motional arm which consists of the series combination of a resistance  $R_1$ , inductance  $L_1$ , and a capacitance  $C_1$ . In the scope of this model, the p-n junction behaves as capacitor when it is at the series resonance mode. In this case, the motional arm's reactance is zero and impedance ( $Z$ ) value is least, this result in maximum ac current flow [17]. On the other hand, at  $f_p$  the  $|Z|$  value of the motional arm is maximal compared to the static one, forcing the device to behave as simple capacitor creating a resonance of high impedance (antiresonance). The frequency of the two arms of the device resonates in a manner to supply high impedance to the current flow [16]. The exchange between the resonance-antiresonance states happened as a result of changes in the effective dielectric constant being unable to accumulate the electromagnetic energy. This action dominates when the incident signal wavelength is larger than the unit cell sizes of the MgO and GaSe<sub>0.5</sub>S<sub>0.5</sub> crystals [18].

The antiresonance condition is used in wave traps that are installed in series with antennas of microwave receivers to block the flow of alternating current at the frequency of an interfering base station, while allowing other frequencies to pass. Recent developments in mobile technology included the invention of resonant-antiresonant devices that oscillate

at frequencies of 2.05 GHz [19]. The bandwidth between the resonance and antiresonance positions of such device is  $\sim 100$  MHz. This property of the Ag/MgO/GaSe<sub>0.5</sub>S<sub>0.5</sub>/Ag device with the very high quality factor makes it attractive for use as microwave resonator and as ultrafast electronic switches that change state in a period of time  $(1/\Delta f) \sim 83$ -10 ns.

The surface acoustic wave (SAW) and bulk acoustic wave (BAW) band pass filters which represent an important part of the market are popularly used in communication technology especially in mobile phones. The SAW device which is simply composed of metallic layer on piezoelectric substrate, is reported to suffer from drawbacks, because they need large area, few millimeters square. They can also handle a limited power and they are limited for the maximum frequency [20]. In addition, the thinner the electrode fingers are, the greater the risk of open or short circuit is. These problems are added to the problem of the possible contamination of the surface. On the other hand, the BAW filters are based on structures where a piezoelectric material is excited in thickness mode and surrounded by metal electrodes. The first structure, film bulk acoustic resonator (FBAR) is realized on a membrane under which an air cavity is created by micro machining to ensure a good acoustic reflection. The main drawbacks of FBAR are the complex process to realize the air cavity and the fragility of the devices. The second structure is Solidly Mounted Resonator (SMR) where the piezoelectric layer and its electrodes are placed on Bragg acoustic reflector. For both structures, a final layer is deposited on the top and its thickness is adjusted to reach the right resonant frequency. These filters have been highly improved compared to SAW filters, however they are reported to remain sensitive to temperature variations and to high power.

The needless for the etching, the very thin crystal layer required for the design (low dimensions), the very high quality of the resonating signal, the ability to work at very high voltages ( $\sim 100$  V) and high frequencies, the cheapness of the design and the needles for mechanical effects make the Ag/MgO/GaSe<sub>0.5</sub>S<sub>0.5</sub>/C device promising element for replacing the SAW and BAW filters.

#### IV. CONCLUSION

The study of the properties of the magnesium oxide and GaSe<sub>0.5</sub>S<sub>0.5</sub> interface has shown the ability of implanting this device as an optoelectronic component which could carry more than one duty at a time. The first, which is presented by the amplification of signals under the laser excitations of 406 and 632 nm, makes the device promising for optical fiber receivers. The second, which is presented by the illumination of the sun spectrum like and the amplification of signals, makes it suitable for use in visible light communications. The third possible duty is to use the device as band stop filter which blocks signals of microwave frequencies.

#### REFERENCES

- [1] H. Li, X. Chen, J. Guo, and H. Chen, "A 550 Mbit/s real-time visible light communication system based on phosphorescent white light LED for practical high-speed low-complexity application," *Opt. Exp.*, vol. 22, no. 22, pp. 27203–27213, 2014.

- [2] N. Fujimoto and H. Mochizuki, "614 Mbit/s OOK-based transmission by the duobinary technique using a single commercially available visible LED for high-speed visible light communications," in *Proc. 38th Eur. Conf. Exhibit. Opt. Commun. (ECOC)*, Sep. 2012, pp. 1–3.
- [3] B. Arredondo *et al.*, "Visible light communication system using an organic bulk heterojunction photodetector," *Sensors*, vol. 13, no. 9, pp. 12266–12276, 2013.
- [4] A. M. Selman, Z. Hassan, M. Husham, and N. M. Ahmed, "A high-sensitivity, fast-response, rapid-recovery p–n heterojunction photodiode based on rutile TiO<sub>2</sub> nanorod array on p-Si(111)," *Appl. Surf. Sci.*, vol. 305, pp. 445–452, Jun. 2014.
- [5] H. K. Khanfar and A. F. Qasrawi, "Performance of the Au/MgO/Ni photovoltaic devices," *Mater. Sci. Semicond. Process.*, vol. 29, pp. 183–187, Jan. 2015.
- [6] H. K. Khanfar, A. F. Qasrawi, and N. M. Gasanly, "Analysis of the junction properties of C/GaSe<sub>0.5</sub>S<sub>0.5</sub>/C back-to-back Schottky-type photodetectors," *IEEE Sensors J.*, vol. 15, no. 4, pp. 2269–2273, Apr. 2015.
- [7] A. F. Qasrawi and N. M. Gasanly, "Energy band diagram and current transport mechanism in p-MgO/n-Ga<sub>4</sub>Se<sub>3</sub>S," *IEEE Trans. Electron Devices*, vol. 62, no. 1, pp. 102–106, Jan. 2015.
- [8] X. H. Xie, Z. Z. Zhang, C. X. Shan, H. Y. Chen, and D. Z. Shen, "Dual-color ultraviolet photodetector based on mixed-phase-MgZnO/i-MgO/p-Si double heterojunction," *Appl. Phys. Lett.*, vol. 101, no. 8, p. 081104, 2012.
- [9] A. F. Qasrawi, S. E. Al Garni, and N. M. Gasanly, "Characterization of the MgO/GaSe<sub>0.5</sub>S<sub>0.5</sub> heterojunction designed for visible light communications," *Mater. Sci. Semicond. Process.*, vol. 39, pp. 377–383, Nov. 2015.
- [10] A. F. Qasrawi and H. K. Khanfar, "Effects of laser excitation and temperature on Ag/GaSe<sub>0.5</sub>S<sub>0.5</sub>/C microwave filters," *J. Electron. Mater.*, vol. 43, no. 9, pp. 3121–3127, 2014.
- [11] A. K. Shukla, *Elements of Optical Communication and Opto Electronics*. New Delhi, India: Laxmi Publications, 2012.
- [12] M. E. Levinshtein, S. L. Rumyantsev, and M. S. Shur, *Properties of Advanced Semiconductor Materials: GaN, AlN, InN, BN, SiC, SiGe*. New York, NY, USA: Wiley, 2001.
- [13] A. S. Sedra and K. C. Smith, *Microelectronic Circuits*. London, U.K.: Oxford Univ. Press, 2004.
- [14] M. S. Tyagi, *Introduction to Semiconductor Materials and Devices*. New York, NY, USA: Wiley, 1988.
- [15] R. H. Bube, *Photoelectronic Properties of Semiconductors*. London, U.K.: Cambridge Univ. Press, 1992.
- [16] F. Léonard and J. Tersoff, "Negative differential resistance in nanotube devices," *Phys. Rev. Lett.*, vol. 85, pp. 4767–4770, Nov. 2000.
- [17] V. E. Bottom, *Introduction to Quartz Crystal Unit Design*. New York, NY, USA: Van Nostrand, 1982.
- [18] T. Koschny, P. Markoš, D. R. Smith, and C. M. Soukoulis, "Resonant and antiresonant frequency dependence of the effective parameters of metamaterials," *Phys. Rev. E*, vol. 68, p. 065602(R), Dec. 2003.
- [19] K. Asai and A. Isobe, "Semiconductor device, manufacturing method of the same, and mobile phone," U.S. Patent 20140018126 A1, Jan. 16, 2014.
- [20] P. Benech and J. M. Duchamp, "Piezoelectric materials and their applications in radio frequency domain and telecommunications," *Adv. Appl. Ceram.*, vol. 114, no. 4, pp. 220–225, 2015.



**Atef F. Qasrawi** was born in Palestine in 1968. He received the B.Sc., M.S., and Ph.D. degrees in physics from Middle East Technical University, Ankara, Turkey, in 1994, 1997, and 2000, respectively. He is currently a Full Professor of Physics with the Department of Physics, Arab American University–Jenin, Jenin, Palestine, and the Physics Group, Atilim University, Ankara. His research includes in most of experimental and computational solid-state physics and electronics. His current research focuses on the design and characterization of microwave tunneling devices and pyrochlore ceramics. He received over 15 researcher awards, and has over 110 Thomson-ISI publications in solid-state physics and electronics. His ISI-citation record exceeded 530 according to the 2014 statistics.



**Hazem K. Khanfar** (M'11) received the M.S. degree in telecommunication and electronics from the Jordan University of Science and Technology, Irbid, Jordan, in 2004, and the Ph.D. degree in electrical engineering from the University of New Orleans, New Orleans, LA, USA, in 2009. He is currently an Assistant Professor with the Faculty of Engineering and IT, Arab American University–Jenin, Jenin, Palestine. His current research interests include thin-film solid states, design of tunneling diodes, and signal processing.



**N. M. Gasanly** received the M.S. degree from Baku State University, Baku, Azerbaijan, in 1963, and the Ph.D. degree from the Physico-Technical Institute, Leningrad, Russia, in 1972. He joined Baku State University in 1972. Since 1992, he has been a Visiting Professor with Middle East Technical University, Ankara, Turkey. He has co-authored 267 scientific papers.